

Numerical analysis of a spontaneous collapse model for a two-level system

Angelo Bassi*

*The Abdus Salam International Centre for Theoretical Physics, Trieste, and
Istituto Nazionale di Fisica Nucleare, sezione di Trieste, Italy.*

Emiliano Ippoliti†

*Department of Theoretical Physics, University of Trieste, and
Istituto Nazionale di Fisica Nucleare, sezione di Trieste, Italy.*

We study a spontaneous collapse model for a two-level (spin) system. The numerical solution of the equations of motions allow to give precise estimates on the regime at which the collapse of the statevector occurs, the reduction and delocalization times, and the reduction probabilities. It allows also to give a clear picture of the transition from the “microscopic” regime (when the noise terms are weak) to the “macroscopic” regime (when the noise terms become dominant).

PACS numbers: 03.65.-w, 02.50.Ey, 02.60.Cb

Stochastic Schrödinger equations find fruitful applications both in the theory of open quantum systems [1, 2, 3, 4] and within collapse models [5, 6, 7, 8, 9, 10, 11, 12, 13, 14, 15]. In the first case, the stochastic terms mimic the effect of the environment on the open system¹. In the second case, non-linear and stochastic terms are added to the standard Schrödinger equation to reproduce — under appropriate conditions — the collapse of the wavefunction²; in this way, it is possible to describe within one single dynamical equation both the quantum properties of microscopic systems and the classical properties of macroscopic objects, and in particular the outcomes of measurement processes.

In this paper, we analyze with numerical techniques the dynamics described by the following stochastic Schrödinger equation in the Hilbert space \mathbf{C}^2 :

$$d|\psi_t\rangle = \left[-i\omega\sigma_x dt + \sqrt{\gamma}(\sigma_z - \langle\sigma_z\rangle) dW_t - \frac{\gamma}{2}(\sigma_z - \langle\sigma_z\rangle)^2 dt \right] |\psi_t\rangle, \quad (1)$$

where $\langle\sigma_z\rangle = \langle\psi_t|\sigma_z|\psi_t\rangle$ and σ_x, σ_z are the usual spin operators; W_t is a standard Wiener process: $\mathbb{E}[dW_t] = 0$ and $\mathbb{E}[dW_t^2] = dt$, and the (positive) parameter γ measures the strength of the coupling between the spin

operator σ_z and W_t . The stochastic dynamics is defined on a probability space $(\Omega, \mathcal{F}, \mathbb{P})$ with the filtration $\{\mathcal{F}_t : t \in [0, \infty)\}$ generated in a standard way by the Wiener process W_t .

Eq. (1) describes the evolution of the spin-wavefunction of a 1/2 spin particle; the dynamics is non-trivial, due to the presence of two competing terms which do not commute: on the one side the Hamiltonian $H = \hbar\omega\sigma_x$, whose effect is to rotate the statevector along the x axis of the Bloch sphere; on the other side, the spin operator σ_z which tends to localize the statevector along one of its two eigenstates $|+\rangle, |-\rangle$. Note that the equation is non-linear and, as a consequence, non-unitary, but it is easy to check that it preserves the norm of $|\psi_t\rangle$.

We will begin our analysis by studying the equation for the statistical operator $\rho(t)$ — describing the ensemble of states each of which evolves according to Eq. (1) — which in this case can be solved exactly; we will give a qualitative description of the evolution of $|\psi_t\rangle$, based on the dynamics for $\rho(t)$. We will next solve Eq. (1) numerically, showing that a much richer quantity of information can be obtained: in particular, we will analyze the regime in which the reduction of the statevector to one of the two eigenstates of σ_z occurs, the reduction probabilities, the delocalization mechanism, and the transition from the “quantum” ($\gamma \ll \omega$) to the “classical” ($\gamma \gg \omega$) regime.

I. THE STATISTICAL OPERATOR

The statistical operator $\rho(t) = \mathbb{E}[|\psi_t\rangle\langle\psi_t|]$ obeys the equation of motion³:

$$\frac{d}{dt}\rho(t) = -i\omega[\sigma_x, \rho(t)] - \gamma[\rho(t) - \sigma_z\rho(t)\sigma_z], \quad (2)$$

³ The dynamical evolution embodied in Eq. (2) has been studied in detail in Ref. [6].

*Electronic address: bassi@ictp.trieste.it

†Electronic address: ippoliti@ts.infn.it

¹ The advantage of this kind of approach over the standard one based on the reduced density matrix of the open system is mainly computational: in some physical situations, it turns out to be computationally easier to solve numerically the stochastic Schrödinger equation and to perform the appropriate averages over different trajectories, rather than solving numerically the equation for the statistical operator.

² More specifically, it has been shown [5] that a particular choice of the stochastic terms exists such that: 1) the quantum properties of microscopic systems are not altered in any appreciable way; accordingly, these models reproduce all experimental results known at present; 2) at the macroscopic level, the reduction mechanism becomes rapidly effective so that macro-objects are always localized in space.

which of course is of the Lindblad type [16]. It can be solved analytically for any given initial condition; if we consider the matrix elements of ρ with respect to the eigenstates $|+\rangle$, $|-\rangle$ of σ_z :

$$\rho \longrightarrow \begin{pmatrix} \langle +|\rho|+\rangle & \langle +|\rho|-\rangle \\ \langle -|\rho|+\rangle & \langle -|\rho|-\rangle \end{pmatrix} = \begin{pmatrix} x & y + iz \\ y - iz & 1 - x \end{pmatrix},$$

we get the following equations for x , y and z :

$$\begin{cases} \dot{x}(t) = -2\omega z(t) \\ \dot{y}(t) = -2\gamma y(t) \\ \dot{z}(t) = -\omega + 2\omega x(t) - 2\gamma z(t). \end{cases} \quad (3)$$

The complete solutions of equations (3) are written in appendix I; here we limit ourselves to discuss some general features.

The equation for $y(t)$ is, trivially, a decaying exponential; the two equations for $x(t)$ and $z(t)$ lead to the following second order differential equation for $z(t)$:

$$\ddot{z}(t) + 2\gamma \dot{z}(t) + 4\omega^2 z(t) = 0, \quad (4)$$

which is the equation of a damped harmonic oscillator; accordingly, for any value of ω and γ (different from zero) the off-diagonal elements of the density matrix decrease exponentially in time. This results would suggest that reductions occur for *any* value of γ — even though, of course, we expect the localization mechanism to be less efficient for smaller values of γ — but we will see in the following sections that the real situation is subtler.

The time evolution of $x(t)$ has the following interesting property: for any value of ω and γ (different from zero) and for any given initial condition, one has that

$$x(t) \xrightarrow[t \rightarrow +\infty]{} \frac{1}{2} \quad (5)$$

This result is interpreted in the following way: suppose that the initial (at time $t = 0$) statevector is, e.g.:

$$|\psi_0\rangle = \sqrt{\frac{3}{4}}|+\rangle + \sqrt{\frac{1}{4}}|-\rangle, \quad (6)$$

and assume that after a certain amount of time it has been stochastically reduced either to the state $|+\rangle$ or to the state $|-\rangle$, with the correct quantum probabilities. As a consequence, the density matrix becomes almost diagonal, with the diagonal elements equal to $3/4$ and $1/4$.

Result (5) states that, as time goes to infinity, the diagonal elements must change and become asymptotically equal to $1/2$: this implies that, however it has been initially reduced, the statevector starts jumping between the two eigenstates, so that after a certain amount of time there is an equal probability of finding it either reduced around $|+\rangle$ or around $|-\rangle$, despite that, at the very beginning, there was a much higher probability to find it reduced around $|+\rangle$. In the following sections we will give a quantitative analysis of this effect.

Note that the above result does not come as a surprise, since a general theorem by Spohn [17] assures that, in the finite dimensional case, when an equation of the quantum dynamical semigroup type admits a steady solution, then any other solution converges to it for $t \rightarrow +\infty$. In our case, equation (2) has $\frac{1}{2}I$ as the only steady solution, where I is the identity matrix: accordingly, the off-diagonal elements must necessarily vanish as time increases, while the diagonal elements must converge to $1/2$.

II. REDUCTION TIMES

The dynamics described by eq. (1) has several interesting properties. The first quantity which we have analyzed is the reduction time, i.e. the time it takes for the statevector to reduce to one of the two eigenstates $|+\rangle$, $|-\rangle$ of the spin operator σ_z . A *reduction process* must satisfy the following two requirements:

1. The statevector $|\psi_t\rangle$ must get “close enough” to one of the eigenstates of the reducing operator, σ_z in our case;
2. Once the statevector reaches such an eigenstate, it must remain close to it for a “sufficiently long” time interval.

Let us make these two requirements more precise. When $|\psi_t\rangle$ gets close to the eigenstate $|+\rangle$ ($|-\rangle$), the square modulus $|\langle +|\psi_t\rangle|^2$ (respectively, $|\langle -|\psi_t\rangle|^2$) approaches the value 1: accordingly, the first requirement amounts to saying that either $|\langle +|\psi_t\rangle|^2$ or $|\langle -|\psi_t\rangle|^2$ is greater than $1 - \varepsilon$, where ε is a parameter depending on the physical situation under study. Following the second requirement, when — let us say — it happens that $|\langle +|\psi_t\rangle|^2 > 1 - \varepsilon$, a reduction has occurred only if this condition holds for a time interval of length τ ; once more, the suitable value for τ depends on the specific physical system.

According to the above arguments, we define the *reduction time* as follows: it is the smallest time t_r such that, for $t \in [t_r, t_r + \tau]$, the square modulus $|\langle +|\psi_t\rangle|^2$ (or $|\langle -|\psi_t\rangle|^2$) is greater than $1 - \varepsilon$.

Fig. 1 shows the results of the numerical simulations for the reduction time as a function of γ , with the initial statevector⁴ $|\psi_0\rangle$ as in eq. (6) and $\omega = 1 \text{ s}^{-1}$. We have taken $\varepsilon = 1/100$, while τ has been chosen according to the following criterion: when $\gamma = 0$ and $|\psi_0\rangle = |+\rangle$ or $|-\rangle$, the statevector rotates between the two eigenstates of σ_z with frequency ω . Accordingly, even if no reducing terms are present, the dynamics brings periodically $|\psi_t\rangle$ close to, e.g., $|+\rangle$, in such a way that $|\langle +|\psi_t\rangle|^2$ remains greater than $1 - \varepsilon$ for a time equal to: $\pi/2 - \arcsin(1 - \varepsilon) \approx$

⁴ In all simulations, we have taken (6) as the statevector at time $t = 0$.

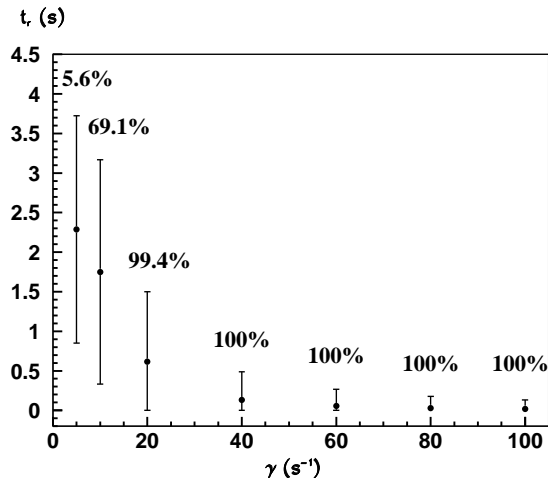


FIG. 1: Reduction time t_r as a function of γ ; the simulations have been made for $\gamma = 5, 10, 20, 40, 60, 80, 100 s^{-1}$, while $\omega = 1 s^{-1}$. The picture shows the average values and the standard deviations over 100.000 trajectories. Above each bar, we have indicated the fraction of the total trajectories which have been reduced within the time interval $[0, 2\pi]$ seconds.

0.141 s. We have then chosen τ to be equal to $10 \times [\pi/2 - \arcsin(1 - \varepsilon)]$, to distinguish a reduction from the effects of the oscillatory motion induced by the Hamiltonian H .

The simulation shows that, as expected, the reduction time decreases for increasing values of γ . When γ is sufficiently larger than ω ($\gamma \geq 60 s^{-1}$), the reduction time becomes a well defined quantity: all trajectories are reduced, and the variance associated to t_r decreases as γ increases⁵. On the other hand, when γ is of the same order of — or smaller than — ω , only a few trajectories (or none) are localized and the variance associated to the reduction times, increases: in this regime, the reduction process progressively disappears. This result is particularly important in relation to the time evolution of the off-diagonal elements of the density matrix.

In the previous section, we have seen that, for *any* value of γ , the off-diagonal elements of the density matrix decrease exponentially in time. According to the numerical simulations of Fig. 1, such a damping has two different origins according to whether γ is significantly greater than ω or not: in the first case, the damping is due to the localization process; in the second case, it is a consequence of a phase randomization (decoherence) of the different trajectories.

This property of eq. (1) is well represented in Figs. 2 and 3. Fig. 2a shows a typical trajectory for the

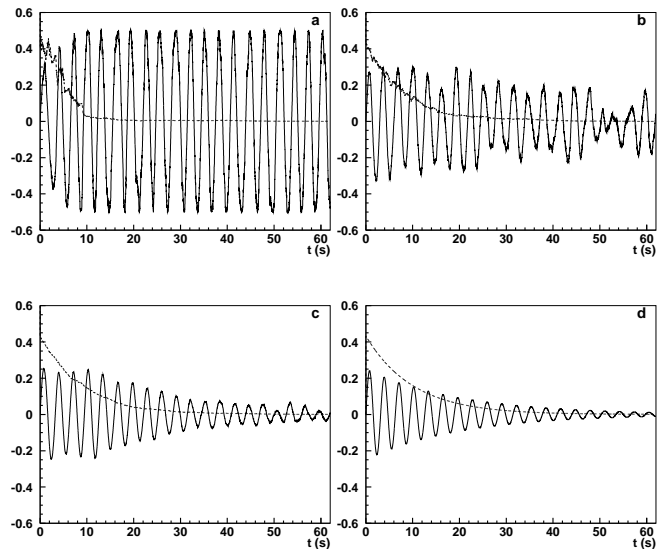


FIG. 2: a) Time evolution of the real (dotted line) and imaginary (continuous line) parts of $\langle +|\psi_t\rangle\langle\psi_t|->$, for a typical trajectory followed by the statevector. The parameter γ has been taken equal to $0.05 s^{-1}$, while as usual $\omega = 1 s^{-1}$. b) and c) show the average values over 5 and 100 different trajectories, respectively. Note the decoherence effect: as time increases, the imaginary parts pick up different random phases and interfere destructively. d) shows the (theoretical) average values, corresponding to the time evolution of the real (y) and imaginary (z) parts of the off-diagonal element $\langle +|\rho(t)|->$ of the density matrix.

real and imaginary parts of $\langle +|\psi_t\rangle\langle\psi_t|->$, when $\gamma = 0.05 s^{-1}$: the real part (dotted line) decreases in time, while the imaginary part (continuous line) oscillates and does not approach the value zero. Figs. 2b and 2c show the average values over 5 and 100 trials, respectively; while the time evolution of the real part of $\langle +|\psi_t\rangle\langle\psi_t|->$ does not change in a significant way, the evolution of the imaginary part displays a typical decoherence effect: the trajectories pick up different random phases and interfere destructively. Decoherence is then responsible of the exponential damping of the off-diagonal element $\langle +|\rho(t)|-> = \mathbb{E}[\langle +|\psi_t\rangle\langle\psi_t|->]$ of the statistical operator, as shown in Fig. 2d.

Fig. 3a, instead, shows the result of the numerical simulations for the (typical) evolution of the real and imaginary parts of $\langle +|\psi_t\rangle\langle\psi_t|->$, when $\gamma = 50 s^{-1}$: both parts are almost always close zero, as an effect of the reduction process. Figs. 3b and 3c show an average over 5 and 100 trials respectively, while Fig. 3d shows the mean value $\langle +|\rho(t)|-> = \mathbb{E}[\langle +|\psi_t\rangle\langle\psi_t|->]$: in this regime, the damping of the off-diagonal elements of the density matrix is not due to a decoherence effect but to the reduction process, since (almost all) realizations of $\langle +|\psi_t\rangle\langle\psi_t|->$ are vanishingly small.

⁵ The mathematical proof that, for $\gamma \gg \omega$, the statevector is reduced to one of the eigenstates of the “reducing operator” (σ_z , in our case), was first given in ref. [5]. See also ref. [15] for a martingale proof.

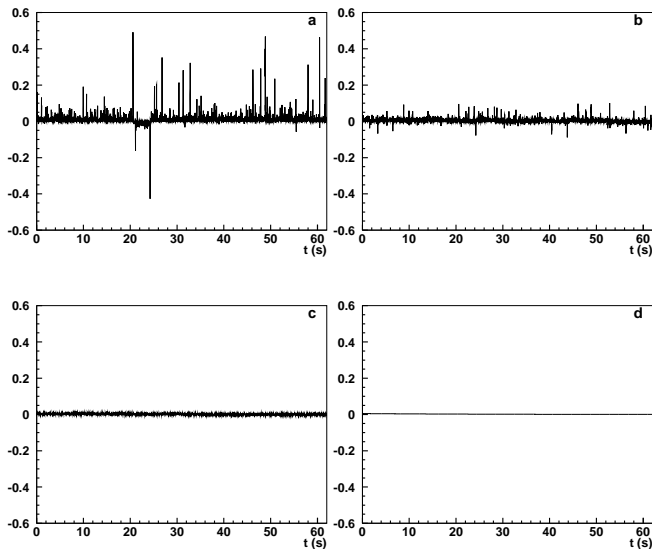


FIG. 3: As in Fig. 2, but with $\gamma = 50 \text{ s}^{-1}$. Only the imaginary parts can be seen, as the real ones go rapidly to zero. Note that the decoherence effect is almost absent: when γ is sufficiently larger than ω , single trajectories share the property that both the real and the imaginary parts of $\langle +|\psi_t\rangle\langle\psi_t|-\rangle$ are (most of the time) close to zero.

III. PROBABILITIES

The second interesting quantity to analyze is the probability that the statevector reduces toward either the eigenstate $|+\rangle$ or the eigenstate $|-\rangle$. The results of the simulation are shown in table I. When γ is much larger than ω , the probability that a reduction occurs approaches the quantum probabilities of finding the value $+1$ or -1 in a measurement of the observable σ_z , given the initial statevector (6):

$$\begin{aligned} \text{Prob.}[\text{reduction near } |+\rangle] &\simeq |\langle +|\psi_0\rangle|^2 = 3/4 \\ \text{Prob.}[\text{reduction near } |-\rangle] &\simeq |\langle -|\psi_0\rangle|^2 = 1/4 \end{aligned}$$

This is an expected result. In fact, by denoting $\alpha_t = \langle +|\psi_t\rangle$ and $\beta_t = \langle -|\psi_t\rangle$, one has from eq. (1):

$$d|\alpha_t|^2 = -2\omega\text{Im}[\alpha_t\beta_t^*]dt + 4\sqrt{\gamma}|\alpha_t|^2(1-|\alpha_t|^2)dW_t \quad (7)$$

and similarly for $|\beta_t|^2$. In the regime $\gamma \gg \omega$, one can neglect ω :

$$|\alpha_t|^2 = |\alpha_0|^2 + 4\sqrt{\gamma} \int_0^t |\alpha_s|^2(1-|\alpha_s|^2)dW_s. \quad (8)$$

Since the integrand in the above equation is bounded between 0 and 1, one can conclude [18] that $|\alpha_t|^2$ is a martingale, which in particular implies that the expectation value $\mathbb{E}[|\alpha_t|^2]$ does not change in time:

$$\mathbb{E}[|\alpha_t|^2] = |\alpha_0|^2; \quad (9)$$

$\gamma \text{ (s}^{-1}\text{)}$	red. near $ +\rangle$	red. near $ -\rangle$	total red.
100	73879 (74%)	26121 (26%)	100000 (100%)
80	74076 (74%)	25924 (26%)	100000 (100%)
60	73748 (74%)	26252 (26%)	100000 (100%)
40	73142 (73%)	26858 (27%)	100000 (100%)
20	70411 (71%)	29033 (29%)	99444 (99%)
10	45862 (66%)	23279 (34%)	69141 (69%)
5	3432 (61%)	2165 (39%)	5597 (6%)

TABLE I: Reduction probabilities as a function of γ . The last column shows the number of times (over 100.000 trials) the statevector has been reduced within the time interval $[0, 2\pi]$ seconds. The second and third columns show the numbers of reductions toward the eigenstate $|+\rangle$ (second column) and $|-\rangle$ (third column).

in other words, reductions (and we have seen that in this regime all trajectories get reduced) occur with the correct quantum probabilities.

On the other hand, when γ is not much larger than ω , the approximation $\omega = 0$ is no longer valid, and the martingale property does not hold any more. As a matter of fact, the numerical simulation shows that, when γ decreases, the reduction probabilities approach the values

$$\begin{aligned} \text{Prob.}[\text{reduction near } |+\rangle] &\simeq 1/2 \\ \text{Prob.}[\text{reduction near } |-\rangle] &\simeq 1/2; \end{aligned}$$

anyway, we have seen in the previous section that for decreasing values of γ , fewer and fewer trajectories are localized, so that the reduction mechanism progressively loses its statistical meaning and eventually disappears.

As a final note, we observe that the term $-2\omega\text{Im}[\alpha_t\beta_t^*]dt$ in Eq. (7) — which spoils the martingale property of $|\alpha_t|^2$ — appears because the standard Hamiltonian $H = \hbar\omega\sigma_x$ and the reduction operator σ_z do not commute. Would they commute, such a term would be zero and $|\alpha_t|^2$ would be a martingale for any value of γ .

IV. DELOCALIZATION TIME

Even when $\gamma \gg \omega$, the fact that the Hamiltonian H does not commute with the reduction operator σ_z has an important effect, which has not always been stressed in the literature: once the statevector has reached one eigenstate, it does not fluctuate around it forever, as there is always the chance that it jumps to the other eigenstate of σ_z . When this occur, we speak of a *delocalization*.

The delocalization time has been defined in the following way: assume that the statevector has been reduced to the eigenstate $|+\rangle$, which amounts to saying that $|\langle +|\psi_t\rangle|^2$ remained larger than $1 - \varepsilon$ for a time interval at least equal to τ . If, starting from any time t_d

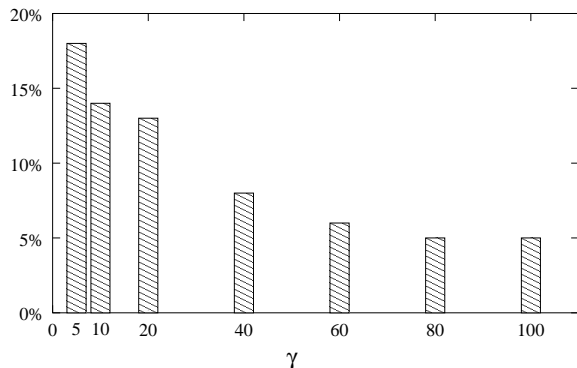


FIG. 4: The picture shows — as a function of $\gamma = 5, 10, 20, 40, 60, 80, 100 \text{ s}^{-1}$ — the fraction of all trajectories (which have suffered a localization) that have been delocalized within the time interval $[t_r, 2\pi]$ seconds.

subsequent to t_r , the square modulus $|\langle +|\psi_t\rangle|^2$ becomes *smaller* than $1 - \varepsilon$ for at least a time interval equal to τ , we say that the statevector has been delocalized from the eigenstate $|+\rangle$ and we call t_d the delocalization time.

Fig. 4 shows the results of the numerical simulation for the delocalization times. We have considered all trajectories which have been localized within the time interval $[0, 2\pi]$ seconds, and we have counted the number of them which have gone through a delocalization within the time interval $[t_r, 2\pi]$, where t_r is the reduction time for each single trajectory. As expected, for increasing values of γ , the fraction of all trajectories which are delocalized before time $t = 2\pi \text{ s}$, decreases: once the statevector gets localized to either one eigenstate of σ_z , it fluctuates around it for a time interval which is longer, the greater the value of γ .

V. TRANSITION FROM THE “MICROSCOPIC” TO THE “MACROSCOPIC” REGIME

We conclude our analysis by giving a general picture of how the evolution of $|\psi_t\rangle$ changes when moving from the “microscopic” ($\gamma \ll \omega$) regime to the “macroscopic” ($\gamma \gg \omega$) one⁶. When γ is vanishing small, the statevec-

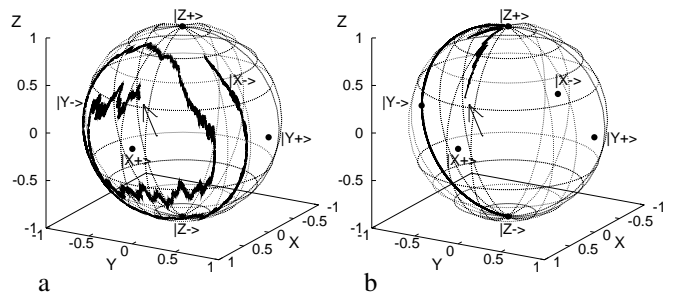


FIG. 5: The figures show two typical trajectories followed by the statevector in the Bloch sphere, for $\gamma = 0.05 \text{ s}^{-1}$ (Fig. a) and $\gamma = 5 \text{ s}^{-1}$ (Fig. b). In the first case, the Hamiltonian H rotates the statevector along the x axis of the Bloch sphere, while the reducing terms slowly move the rotation plane towards the $|+\rangle$ and $|-\rangle$ eigenstates. In the second case, the effect of the reduction terms is so strong that the statevector is rapidly driven towards the $|+\rangle$ eigenstate and then fluctuates around it, until it jumps to the other eigenstate $|-\rangle$. The arrows mark the starting point of the trajectories.

tor simply rotates along the x -axis of the Bloch sphere, guided by the standard Hamiltonian $H = \hbar\omega\sigma_x$. As γ increases — still remaining smaller than ω — $|\psi_t\rangle$ keeps rotating along the x -axis, but the stochastic terms shift the rotation plane towards the two eigenstates of σ_z (see fig. (5a)).

When γ becomes significantly greater than ω , the statevector does not rotate anymore around the x -axis of the Bloch sphere: it gets rapidly reduced to one of the two eigenstate of σ_z (see fig. (5b)); moreover, if γ is sufficiently large, the reductions occur with the correct quantum probabilities.

The statevector then fluctuates around the eigenstate to which it has been reduced for a time interval that — statistically — is longer, the greater the values of γ ; accordingly, when ω can be neglected, the system behaves like a macroscopic system (regarding the physical properties of the spin along the z -axis): the operator σ_z always has a well definite value.

Acknowledgements

We acknowledge many useful discussions with prof. G.C. Ghirardi. We also thank prof. S. Baroni for having introduced us to the field of numerical simulations of stochastic differential equations.

⁶ In collapse models [5], the parameter γ is constant and much smaller than the inverse of the characteristic times of the free Hamiltonian, so that microscopic systems are weakly coupled to the stochastic terms; this is the reason why the $\gamma \ll \omega$ regime has been called “microscopic”. On the other hand, it can be proved that macroscopic objects strongly interact with the noise terms: in fact, the effects of such terms on the constituents of the macro-system sum with each other, in such a way that the dynamics of the object is governed by an effective single-particle collapse-equation, with a γ much great than the inverse of the characteristic times of the free Hamiltonian. It is precisely this strong interaction which is responsible for their classical behavior. Accordingly, the $\gamma \gg \omega$ regime has been called “macro-

scopic”.

Appendix I: complete solutions of the equation for the statistical operator

The solutions of equations (3) are:

Over-damped case: $\gamma > 2\omega$.

$$\begin{aligned} x(t) &= a e^{-\gamma(1+\mu)t} + b e^{-\gamma(1-\mu)t} + 1/2 \\ y(t) &= y_0 e^{-2\gamma t} \\ z(t) &= c e^{-\gamma(1-\mu)t} + d e^{-\gamma(1+\mu)t}, \end{aligned} \quad (10)$$

with:

$$\begin{aligned} a &= -\frac{2\omega^2}{\gamma^2\mu(1+\mu)}x_0 + \frac{\omega}{\gamma\mu}z_0 + \frac{\omega^2}{\gamma^2\mu(1+\mu)} \\ b &= \frac{2\omega^2}{\gamma^2\mu(1-\mu)}x_0 - \frac{\omega}{\gamma\mu}z_0 - \frac{\omega^2}{\gamma^2\mu(1-\mu)} \\ c &= -\frac{\omega}{\gamma\mu}x_0 + \frac{1+\mu}{2\mu}z_0 + \frac{\omega}{2\gamma\mu} \\ d &= \frac{\omega}{\gamma\mu}x_0 - \frac{1-\mu}{2\mu}z_0 - \frac{\omega}{2\gamma\mu} \\ \mu &= \sqrt{1 - \left(\frac{2\omega}{\gamma}\right)^2} \end{aligned} \quad (11)$$

Critically damped case: $\gamma = 2\omega$.

$$\begin{aligned} x(t) &= [a + bt]e^{-\gamma t} + 1/2 \\ y(t) &= y_0 e^{-2\gamma t} \\ z(t) &= [c + dt]e^{-\gamma t}, \end{aligned} \quad (12)$$

with:

$$\begin{aligned} a &= x_0 - \frac{1}{2} \\ b &= (2x_0 - 1)\omega - \gamma z_0 \\ c &= z_0 \\ d &= (2x_0 - 1)\omega - \gamma z_0. \end{aligned} \quad (13)$$

Under-damped case: $\gamma < 2\omega$.

$$\begin{aligned} x(t) &= [a \cos(\lambda t) + b \sin(\lambda t)]e^{-\gamma t} + 1/2 \\ y(t) &= y_0 e^{-2\gamma t} \\ z(t) &= [c \cos(\lambda t) + d \sin(\lambda t)]e^{-\gamma t}, \end{aligned} \quad (14)$$

with:

$$\begin{aligned} a &= x_0 - \frac{1}{2} \\ b &= \frac{\gamma}{\lambda}x_0 - \frac{2\omega}{\lambda}z_0 - \frac{\gamma}{2\lambda} \\ c &= z_0 \\ d &= \frac{1}{\lambda}(2\omega x_0 - \omega - \gamma z_0) \\ \lambda &= \gamma \sqrt{\left(\frac{2\omega}{\gamma}\right)^2 - 1} \end{aligned} \quad (15)$$

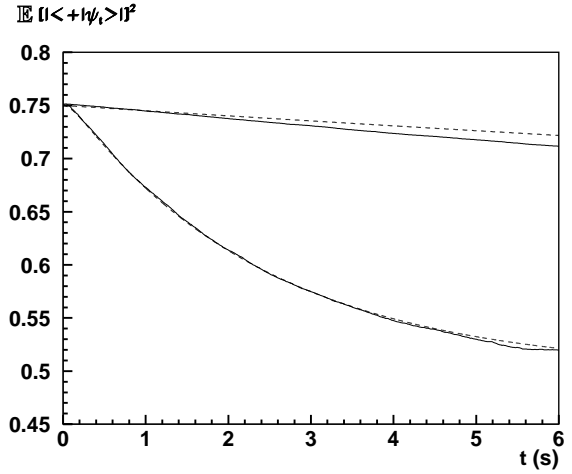


FIG. 6: The two dotted curves represent the (analytical) evolution $\langle +|\rho(t)|+ \rangle$, with $\gamma = 100 \text{ s}^{-1}$ (upper curve) and $\gamma = 5 \text{ s}^{-1}$ (lower curve). The continuous curves show the average value of $|\langle +|\psi_t \rangle|^2$ over 100.000 trajectories of $|\psi_t \rangle$, for the same values of γ . For the values of the time step, see the text.

Appendix II: a note on the numerical simulation

To solve eq. (1), we have used the simple Euler algorithm, which proved to be satisfactory for the purposes of the article. To test the goodness of the simulation, we have compared⁷ the analytical evolution of $\mathbb{E}[|\langle +|\psi_t \rangle|^2] = \langle +|\rho(t)|+ \rangle$ with the average value of $|\langle +|\psi_t \rangle|^2$ over many sample trajectories, obtained by solving eq. (1) numerically (see Fig. 6).

While analyzing the data, we have seen that for large values of γ — i.e. when the reduction mechanism becomes extremely rapid — the numerical simulation was not as good as expected. For such a reason we have decided to decrease the time step during the first 0.1 s, obtaining a sensible improvement.

We have made different tests on the choice of the time steps and number of trials and, taking also into account the time required by our CPU for elaborating the data, we have found that the best choice (according to the previously mentioned criterion) was to take:

$$\begin{aligned} \text{Time step for } t \leq 0.1 \text{ s:} & \quad 10^{-7} \\ \text{Time step for } t > 0.1 \text{ s:} & \quad 10^{-3} \\ \text{Number of trials:} & \quad 100.000. \end{aligned}$$

⁷ Of course, such a comparison tests the convergence of the numerical algorithm in the *weak* sense (i.e. in the mean) [19], while a test for the convergence in the *strong* sense (for single trajectories) would have been better; but this kind of a test is not feasible. Note that Euler scheme is of order 1 for the convergence in the weak sense, while it is of order 1/2 for the convergence in the strong sense.

-
- [1] E.B. Davies, “Quantum theory of open systems”, London Academic Press (1976).
- [2] D. Giulini, E. Joos, C. Kiefer, J. Kupsch, I.-O. Stamatescu and H.D. Zeh, *Decoherence and the Appearance of a Classical World in Quantum Theory*, Springer (1996).
- [3] M.B. Plenio and P.L. Knight, *Rev. Mod. Phys.* **70**, 101 (1998).
- [4] H.P. Breuer and F. Petruccione, “The theory of open quantum systems”, Oxford University Press (2002).
- [5] G. C. Ghirardi, P. Pearle and A. Rimini, *Phys. Rev. A* **42**, 78 (1990). G.C. Ghirardi, R. Grassi and P. Pearle, *Found. Phys.* **20**, 1271 (1990). G.C. Ghirardi, R. Grassi and A. Rimini, *Phys. Rev. A* **42**, 1057 (1990). G.C. Ghirardi, R. Grassi and F. Benatti, *Found. Phys.* **25**, 5 (1995).
- [6] G.C. Ghirardi, *Phys. Lett. A* **262**, 1 (1999).
- [7] P. Pearle, *Phys. Rev. D* **13**, 857 (1976). *Phys. Rev. Lett.* **53**, 1775 (1984). *Phys. Rev. A* **39**, 2277 (1989).
- [8] L. Diósi, *Phys. Lett. A* **132**, 233 (1988). *J. Phys. A* **21**, 2885 (1988). *Phys. Rev. A* **40**, 1165 (1989). *Phys. Rev. A* **42**, 5086 (1990).
- [9] V.P. Belavkin, in *Lecture Notes in Control and Information Science* **121**, A. Blaquièrè ed., 245 (1988). V.P. Belavkin and P. Staszewski, *Phys. Lett. A* **140**, 355 (1989). *Phys. Rev. A* **45**, 1347 (1992).
- [10] A. Barchielli, *Quantum Opt.* **2**, 423 (1990). *Int. J. Theor. Phys.* **32**, 2221 (1993).
- [11] Ph. Blanchard and A. Jadczyk, *Phys. Lett. A* **175**, 157 (1993). *Ann. der Physik* **4**, 583 (1995). *Phys. Lett. A* **203**, 260 (1995).
- [12] N. Gisin and J. Percival, *Phys. Lett. A* **167**, 315 (1992). *J. Phys. A* **26**, 2233 (1993); **26**, 2243 (1993). N. Gisin and I. Percival, *Journ. Phys. A* **25**, 5677 (1992). N. Gisin and M. Rigo, *Journ. Phys. A* **28**, 7375 (1995).
- [13] I. Percival, *Quantum State Diffusion*, Cambridge University Press, Cambridge (1998).
- [14] L.P. Hughston, *Proc. R. Soc. London A* **452**, 953 (1996).
- [15] S.L. Adler and L.P. Howritz: *Journ. Math. Phys.* **41**, 2485 (2000). S.L. Adler and T.A. Brun: *Journ. Phys. A* **34**, 4797 (2001). S.L. Adler, D.C. Brody, T.A. Brun and L.P. Hughston, *Journ. Phys. A* **34**, 8795 (2001). S.L. Adler, *Journ. Phys. A* **35**, 841 (2002).
- [16] G. Lindblad, *Commun. Math. Phys.* **48**, 119 (1976).
- [17] H. Spohn, *Rev. Mod. Phys.* **53**, 569 (1980).
- [18] L. Arnold, “Stochastic Differential Equations: Theory and Applications”, Wiley (1971).
- [19] P.E. Kloeden and E. Platen, “Numerical Solutions of Stochastic Differential Equations”, Springer-Verlag, Berlin (1992).